


Drug Delivery System Based On Minoxidil Nanoparticles Promotes Hair Growth In C57BL/6 Mice

This article was published in the following Dove Press journal:
International Journal of Nanomedicine

Noriaki Nagai¹
Yoshie Iwai¹
Akane Sakamoto¹
Hiroko Otake¹
Yoshihiro Oaku¹ ²
Akinari Abe²
Tohru Nagahama²

¹Faculty of Pharmacy, Kindai University, Osaka 577-8502, Japan; ²Research & Development Laboratories Self-Medication, Taisho Pharmaceutical Co., Ltd., Saitama 331-9530, Japan

Purpose: We designed formulations based on minoxidil (MXD) nanoparticles (N-MXD) and examined whether N-MXD can increase drug delivery into the follicles. In addition, we investigated the effect of N-MXD on hair growth in C57BL/6 mice.

Methods: N-MXD (1%) was prepared as follows: methylcellulose, p-hydroxyalkylbenzoates, mannitol, and MXD were dispersed in purified water and milled using zirconia beads under refrigeration (5500 rpm, 30 s×15 times, intermittent milling). C57BL/6 mice were used to evaluate hair-growth effects. The expression levels of mRNA and protein for vascular endothelial growth factor (VEGF) and insulin-like growth factor-1 (IGF-1) were determined by real-time PCR and ELISA methods, respectively.

Results: The ratio of solid-MXD was approximately 60% in N-MXD, and the MXD nanoparticles (90–300 nm) were oblong in shape. For the design of nanomedicines, usability is important. Therefore, we measured the stability and toxicity after N-MXD treatment. No agglutination of MXD nanoparticles was detected for 2 weeks, and no redness or MXD powder residue was observed in the skin after repetitive applications of N-MXD. Next, we evaluated hair-growth effects by N-MXD treatment. MXD contents in the skin tissue from N-MXD were lower than for commercially available MXD formulations (CA-MXD). Conversely, MXD contents in the hair bulbs were higher for N-MXD than for CA-MXD, and the drug efficacy of N-MXD was also higher than that of CA-MXD. In addition, the mRNA and protein levels of IGF-1 and VEGF were enhanced by the repetitive application of N-MXD and CA-MXD, and the enhanced IGF-1 and VEGF levels were significantly higher for N-MXD than for CA-MXD.

Conclusion: We designed a novel nanomedicine based on MXD nanoparticles and showed that N-MXD can deliver MXD into hair bulbs via hair follicles and that the therapeutic efficiency for hair growth is higher than for CA-MXD (solution type).

Keywords: minoxidil, nanoparticle, androgenetic alopecia, hair follicle delivery, hair growth

Plain Language Summary

Minoxidil (MXD) is a drug widely used as therapy for androgenetic alopecia. In this study, we designed formulations based on MXD nanoparticles (1% N-MXD) following the bead mill method and investigated the effect on hair growth using C57BL/6 mice. The particle size of N-MXD was in the range of 90–300 nm. The MXD content in the skin of MDX-applied mice was lower than in the skin of commercially available MXD-applied mice (CA-MXD), but the MXD content in the hair bulbs was higher in N-MXD than in CA-MXD. Moreover, the drug efficacy in N-MXD was significantly higher than in CA-MXD, and the IGF-1 and VEGF levels related to hair growth were also greater in N-MXD than in CA-MXD. In

Correspondence: Noriaki Nagai
Faculty of Pharmacy, Kindai University,
3-4-1 Kowakae, Higashi-Osaka, Osaka
577-8502, Japan
Tel +81 6 4307 3640
Fax +81 6 6730 1394
Email nagai_n@phar.kindai.ac.jp

conclusion, our study shows that N-MXD can deliver MXD directly into hair bulbs via hair follicles, and the therapeutic efficiency on hair growth is higher than that of CA-MXD.

Introduction

Androgenetic alopecia (AGA) is a chronic problem of hair loss observed in both men and women. In particular, it affects up to 50% of the middle-aged males and 95% of 80-year-old men.¹ This hair loss perturbs self-esteem, and this decrease in self-esteem may lead to dissatisfaction and depression. In the treatment of AGA, finasteride and its derivatives are approved and currently used,² while Minoxidil (MXD), a vasodilator, is the most commonly used drug used as therapy for AGA. MXD exerts a vasodilator effect on hair follicles by leading directly to the proliferation of dermal papilla cells.³ However, MXD also shows adverse effects such as inflammation, redness, itching, which limit treatment since the recommended long-term treatment involves twice a day application. In addition, the water solubility of MXD is poor, and the majority of commercially available (CA) formulations are dissolved using propylene glycol (PG) and/or ethanol; for example, a mixture solvent of PG/water/ethanol (20/30/50, v/v/v) is the vehicle for a marketed MXD formulation (solution type, Rogaine, Pfizer). This PG/water/ethanol vehicle can dissolve MXD at levels that allow for effective hair growth, but the organic solvents can lead to allergic contact dermatitis, redness, burning, irritation, and scalp dryness.⁴⁻⁶ Because of these problems, new drug delivery systems (DDS) that target lesions and novel formulations without organic solvents are required to decrease the adverse effects and optimize AGA therapy.⁷

Skin is a natural barrier that acts to inhibit the penetration of particles and exogenous aggressions. However, therapeutic nanoparticles can be delivered to hair follicle openings and into diseased skin.⁸⁻¹⁰ Therefore, nanoparticles may provide a useful strategy for drug delivery to hair follicles. In recent years, lipid nanoparticles have been introduced as potential alternatives to other DDS, such as emulsions, liposomes, and polymeric nanoparticles.¹¹ Aljuffali et al designed lipid nanocarriers with anti-platelet-derived growth factor receptor β antibody to target dermal papilla cells and showed enhanced uptake of MXD.¹² Strategies to deliver MXD into hair follicles have also been reported. Gelfuso et al showed that the microencapsulation and iontophoresis can act synergistically to

enhance topical drug targeting to hair follicles using MXD.¹³ In addition, their group designed chitosan nanoparticles of MXD and showed the chitosan nanoparticles appear to represent a promising and easy strategy to target and sustain drug delivery to hair follicles.^{14,15} Furthermore, Padois et al reported that solid lipid nanoparticles, formulated using physiological lipids in a solvent-free process, are totally non-corrosive to skin, and the formulation should increase patient compliance.⁷ On the other hand, our research group has also developed nanoparticles (NPs) by the combination of methylcellulose (MC) and bead mill treatment,^{16,17} and reported that drug NPs allow for high skin permeation by enhancing the solubility and size of drugs.^{18,19} In addition, drug formulations based on NPs prevent skin stimulation, since NPs avoid the use of organic solvents, such as PG and ethanol for preparation.¹⁸⁻²⁰ Therefore, an MXD formulation based on NPs may reduce the adverse effects and enhance the therapeutic efficacy of MXD.

Mouse models are used most often for studies of hair growth owing to specific mutants, such as rhino, hairless, and nude, and the availability of large databases. In particular, C57BL/6 mice have been widely used to evaluate hair-growth effects. The dorsal hair of C57BL/6 mice has a time-synchronized growth cycle²¹ and truncal pigmentation that is produced only during the anagen phase of hair growth.²² In this study, we designed formulations based on MXD NPs (N-MXD) and examined whether N-MXD can increase drug delivery into the follicles. In addition, we investigated the effect of N-MXD on hair growth in C57BL/6 mice as a model to determine hair-growth effects.

Materials And Methods

Animals And Chemicals

Male 7-week-old C57BL/6 mice were purchased from Clea Japan, Inc. (Tokyo, Japan), and the dorsal hair was removed before use in experiments to evaluate hair follicle delivery and hair-growth effect of MDX. All mice were housed under normal conditions [room temperature 25°C; light/dark time=12-hr cycle; food (CE-2 formulation diet, Clea Japan, Inc., Tokyo, Japan) and free access to water]. The animal experiments were carried out in accordance with the Pharmacy Committee Guidelines for the Care and Use of Laboratory Animals in Kindai University (project identification code KAPS-29-007, 1 April 2017). Conventional

MXD powder, methyl p-hydroxybenzoate, propyl p-hydroxybenzoate, and mannitol were purchased from Wako Pure Chemical Industries, Ltd. (Osaka, Japan), and trizol reagent was obtained from Life Technologies Inc. (Rockville, USA). A vascular endothelial growth factor (VEGF) ELISA kit and Mouse/Rat insulin-like growth factor-1 (IGF-1), and an immunoassay ELISA kit were provided by Cosmo Bio Co., Ltd. (Tokyo, Japan) and R&D systems (Minneapolis, MN, USA), respectively. The commercially available MXD formulation (CA-MXD, Riup 1%) was purchased from Taisho Pharmaceutical Co., Ltd. (Tokyo, Japan). MC was obtained from Shin-Etsu Chemical Co., Ltd. (Tokyo, Japan). A Bio-Rad Protein Assay Kit and RNA PCR Kit (AMV Ver 3.0) were provided by Bio-Rad Laboratories (Hercules, CA, USA) and Takara Bio Inc. (Shiga, Japan), respectively. LightCycler FastStart DNA Master SYBR Green I was purchased from Roche Diagnostics Applied Science (Mannheim, Germany). All other chemicals used were of the highest purity commercially available.

Preparation Of Formulations Based On MXD NPs

Bead mill treatment of MXD was performed using a Bead Smash 12 (Wakenyaku Co. Ltd, Kyoto, Japan) and zirconia beads (diameter: 0.1 mm) according to our previous reports of Nagai.^{16-20,23} Briefly, powder mixtures consisting of MXD, methylcellulose (MC), methyl p-hydroxybenzoate, propyl p-hydroxybenzoate, and mannitol were mixed in 2 mL tubes with zirconia beads. After that, purified water was added to the tube, and the dispersions containing MXD in the tube were set on the Bead Smash 12, and milled under refrigeration (4°C). The milling conditions were 5500 rpm for 30 s, and repeated 15 times (intermittent milling). The milled MXD dispersion was used as N-MXD (MXD formulations containing MXD NPs). In this study, we also prepared a dispersion containing MXD powder, MC, methyl p-hydroxybenzoate, propyl p-hydroxybenzoate, and mannitol and defined it as P-MXD [MXD formulation containing MXD powder (micronized drug)]. The compositions of P-MXD and N-MXD were as follows: MXD 1%, methyl p-hydroxybenzoate 0.026%, propyl p-hydroxybenzoate 0.014%, mannitol 0.5%, MC 2%. The functions of the additives are as follows:¹⁶ MC enhances the crushing efficiency in the bead mill. Methyl p-hydroxybenzoate and propyl p-hydroxybenzoate are parabens and used as preservatives. Mannitol was added to prevent cell stimulation.

The viscosities of the P-MXD, N-MXD, and CA-MXD were 1.88, 1.91, and 1.19 Pa·s at 20°C, respectively.

Measurement Of Particle Size And Number, And Images Of MXD Particles

The particle sizes of the MXD powder and NPs were measured by a particle size analyzer SALD-7100 (Shimadzu Corp., Kyoto, Japan). The refractive index in the SALD-7100 was set at 1.60-0.010i. In addition, the size and number of NPs in N-MXD were detected by NANOSIGHT LM10 (QuantumDesign Japan, Tokyo, Japan) with the measurement conditions set as follows: viscosity of the suspension; 0.904 mPa·s-0.906 mPa·s, wavelength 405 nm, time 60 s. An atomic force microscope (AFM) image was obtained using a scanning probe microscope (SPM)-9700 (Shimadzu Corp., Kyoto, Japan), and the AFM image was created by combining phase and height images. The zeta potential was evaluated using a Zeta Potential Meter Model 502 (Nihon Rufuto Co., Ltd., Tokyo, Japan).

Measurement Of MXD Levels By HPLC Method

An LC-20AT system (HPLC, Shimadzu Corp., Kyoto, Japan) was used to measure the MXD with 1 µg/mL ethyl p-hydroxybenzoate was selected as an internal standard. The mobile phase was methanol/purified water containing 3 mM docusate sodium (1/1, v/v) at a flow rate of 0.2 mL/min. Samples (10 µL) were injected and sent to the detector through a 2.1 mm × 50 mm Inertsil[®] ODS-3 column (GL Science Co., Inc., Tokyo, Japan) at 35°C. MXD was detected at a wavelength of 254 nm.

Measurement Of MXD Levels In The Hair Bulb, Skin Tissue, And Blood

On the day before the experiment, the hair in the dorsal area was carefully cut to a length of approximately 2 mm with an electric clipper and electric razor. The following day, the skin surface was washed with saline, and the MXD was applied. The rats were restrained for about 3 mins after application to prevent them from running around, and then immediately occluded with adhesive tape. Thirty microliters of MXD formulation were applied to the dorsal area (2 cm×2 cm, 4 cm²) of C57BL/6 mice, and left for 4 hrs. After that, the C57BL/6 mice were killed by injection of a lethal dose of pentobarbital, and hair bulbs, skin tissue, and blood were taken. The hair was

collected with tweezers, and the hair bulb area was isolated. The hair bulb and skin tissues were homogenized in ethanol, and the homogenates and blood were centrifuged at 20,400 g for 20 mins at 4°C. The MXD levels in the supernatants were measured by the HPLC method described earlier. In this study, the MXD contents in the hair bulb and skin tissue are represented as/mg protein, and the total protein levels were measured using a Bio-Rad Protein Assay Kit.

Measurement Of Hair-Growth Effect

Thirty microliters of MXD formulation were applied repetitively to the dorsal area (2 cm×2 cm, 4 cm²) of C57BL/6 mice once a day (11:00 a.m.), and hair growth was monitored daily using a digital camera (10:00 a.m.). The change in area with hair (hair zone) was evaluated with image analyzing software Image J, and the area under the hair zone-time curve (AUC) was analyzed according to the trapezoidal rule up to the last measurement point (15 d). In addition, the surface and a cross-section of C57BL/6 mouse skin treated with MXD formulation were also monitored using a digital camera and digital microscope (Bio Medical Science Inc., Tokyo, Japan), respectively.

Quantitative Real-Time Reverse Transcription (RT)-Polymerase Chain Reaction (PCR)

Thirty microliters of MXD formulation were applied repetitively to the dorsal area (2 cm×2 cm, 4 cm²) of C57BL/6 mice for 10 days (once a day, 11:00 a.m.). After that, the C57BL/6 mice were killed by injection of a lethal dose of pentobarbital, and the hair bulbs in the area to which the MXD was applied were removed (3:00 p.m.). Total RNA in the hair bulbs was extracted by the acid guanidinium thiocyanate-phenol-chloroform extraction method using Trizol reagent. The RT and PCR reactions were performed using an RNA PCR Kit and LightCycler FastStart DNA Master SYBR Green I according to the manufacturer's instructions. Briefly, 1 µg of total RNA was mixed with buffer (pH 8.3) comprising Tris (10 mM), MgCl₂ (5 mM), and KCl (50 mM), and mixed with an oligo dT-adaptor primer RNase inhibitor, reverse transcriptase, and deoxynucleotide triphosphate. After that, the mixture was incubated at 42°C for 15 mins, followed by 5 mins at 95°C, and the cDNA was prepared (total 10 µL). Two microliters of cDNA were mixed with 2 µL of LightCycler FastStart DNA Master SYBR Green I Reaction Mix and reaction mixture. After that, the following components were added to give a

final volume of 20 µL: 10 pmol-specific primers for IGF-1 (FOR 5'-CTGGTCCTGTGTCCTTTGC-3, REV 5'-GGACGGGGACTTCTGAGTCTT-3), VEGF (FOR 5'-CAACTCTGGGCTCTTCTCG-3, REV 5'-CCTCTCCTTCTTCTCTCTTCC-3), or glyceraldehyde-3-phosphate dehydrogenase (GAPDH) (FOR 5'-TGCACCACCAACTGCTTAGC-3, REV 5'-GGCATGGACTGTGGTCATGAG-3). The PCR conditions were 95°C for 10 mins, 50 cycles of denaturing (95°C for 10 s), annealing [66°C (IGF-1), 64°C (VEGF), 66 or 64°C (GAPDH) for 10 s], and extension (72°C for 5 s). The differences in the threshold cycles for GAPDH and other groups (IGF-1 and VEGF) were used to calculate the expression levels of IGF-1 mRNA and VEGF mRNA in C57BL/6 mice.

Measurement Of IGF-I Protein In Hair Bulb

Thirty microliters of MXD formulation were applied repetitively to the dorsal area (2 cm×2 cm, 4 cm²) of C57BL/6 mice for 10 days (once a day, 11:00 a.m.). After that, the mice were killed by injecting a lethal dose of pentobarbital, and the hair bulbs in the area to which MXD was applied were taken (3:00 p.m.). IGF-1 levels were measured using a Mouse/Rat IGF-1 Immunoassay ELISA kit according to the manufacturer's instructions. Briefly, the hair bulb sample was homogenized in purified water and centrifuged at 20,400 g for 20 mins (4°C). The supernatant was mixed with Calibrator diluent RD and added to the wells of microplates pre-coated with monoclonal antibodies specific for Mouse IGF-1. The microplates were then incubated for 2 hrs at room temperature and washed 5 times with Wash Buffer. Mouse IGF-1 conjugate reagent was added into the wells, and the plates were incubated for 2 hrs at room temperature. Then, the detection reagent was added, and the plates were incubated for 30 mins at room temperature; the absorbance was measured with a microplate reader at 450 nm.

Measurement Of VEGF Protein In Hair Bulbs

Thirty microliters of MXD formulation were applied repetitively to the dorsal area (2 cm×2 cm, 4 cm²) of C57BL/6 mice for 10 days (once a day, 11:00 a.m.). After that, the mice were killed by injecting a lethal dose of pentobarbital, and the hair bulbs in the area to which MXD was applied were taken (3:00 p.m.). The VEGF levels were measured using a VEGF ELISA kit according to the

manufacturer's instructions. Briefly, the hair bulb sample was homogenized in purified water and centrifuged at 20,400 g for 20 mins (4°C). The supernatant was added into the wells of microplates pre-coated with monoclonal antibodies specific for Mouse VEGF. After that, the microplates were incubated for 2 hrs at 37°C in a humid environment and washed 4 times with Wash Buffer. The detection antibody solution reagent was added into the wells, incubated for 1 hr at 37°C in a humid environment, and washed 4 times with Wash Buffer. Then, horseradish peroxidase (HRP)-conjugate antibody was added to the wells, and the microplates were incubated for 1 hr at 37°C in a humid environment. Next, the microplates with 3,3',5,5'-Tetramethylbenzidine (TMB) substrate solution for HRP were incubated for 15 mins at 37°C in the dark. The absorbance was measured with a microplate reader at 450 nm.

Characterization Of MXD By Powder X-ray Diffraction (XRD) Method

The bead mill treated and not treated MXD preparations were lyophilized and used as samples in XRD using a Mini Flex II (Rigaku, Co., Tokyo, Japan). The X-ray conditions were as follows: 15 mA and 30 kV, and data were obtained from 5° to 90° diffraction angles with a scanning rate of 10°/min.

Statistical Analysis

Data are expressed as the mean \pm standard error (S.E.) of the mean, and Student's *t*-tests and Dunnett's multiple comparison (ANOVA) were used for statistical analysis.

Results

Design Of A Nano-Formulation For The Effective Hair Follicle Delivery Of MXD

Figure 1 shows the size characteristics and solubility of P-MXD and N-MXD. The particle size in P-MXD is in the micro order with a range of 0.4–20 μ m (Figure 1A). P-MXD was crushed by the bead mill method to bring the MXD into the nano order with a range of 90–300 nm (Figure 1B and 1C). The ratio of solid MXD was 61.2% in the N-MXD (38.8% MXD is solution type, Figure 1D), and the morphology of MXD did not differ with or without bead mill treatment since the crystal structure was similar in both preparations (Supplemental data 1). In addition, we measured the form, number and zeta potential of MXD in N-MXD. Visually, the N-MXD formulation is a nebulous

solution (Figure 2A), and the MXD NPs appear oblong in the AFM image (Figure 2B). The particle number was $2.65 \pm 0.28 \times 10^9$ particles/mL, and the zeta potential in was -9.93 mV. For the design of nanomedicines, stability is very important. The particle frequency in N-MXD was similar between samples immediately after preparation and 2 weeks later (Supplemental data 2A), and no agglutination of MXD NPs was observed for 2 weeks (mean particle size by NANOSIGHT LM10, 167 ± 6.8 nm). However, the particle size did increase over the next 2 weeks, and the mean particle size 4 weeks after preparation was 294 ± 9.5 nm (Supplemental data 2B). Therefore, we used freshly prepared N-MXD formulations in all experiments. In this study, we observed the skin surface after the application of N-MXD. Although an MXD powder residue was observed on the surface of mouse skin to which the M-MXD formulation was applied, no residue was observed on skin to which the N-MXD formulation was applied (Figure 2C). Furthermore, there was no skin redness (inflammation) observed for mice treated with N-MXD (Figure 2C).

Effect Of MXD Formulations On Hair-Growth Effect In The C57BL/6 Mice

It is important to deliver the MXD into the hair bulb for effective therapy for AGA. Therefore, we measured the MXD contents in the hair bulb, skin tissue, and blood 4 hrs after the application of MXD formulations (Figure 3). The MXD contents in the hair bulb of mice treated with N-MXD were higher than in mice treated with P-MXD or CA-MXD by 6.0-fold and 1.8-fold, respectively (Figure 3A). In contrast to the results for hair bulb, the MXD contents in the skin tissue were significantly lower in mice treated with N-MXD than with CA-MXD (Figure 3B). In addition, MXD was detected in the blood of mice treated with CA-MXD, although, no plasma MXD was detected following the application of P-MXD or N-MXD (Figure 3C). Moreover, we investigated whether N-MXD promotes hair growth in C57BL/6 mice (Figures 4 and 5). Hair growth was significantly promoted by the application of CA-MXD and N-MXD in comparison with Vehicle, and the drug efficacy of N-MXD was significantly higher than that of P-MXD or CA-MXD. The AUC for N-MXD was 1.38-fold higher than that for Vehicle. Moreover, no redness or skin inflammation was observed after the repetitive application of N-MXD (Figure 4A).

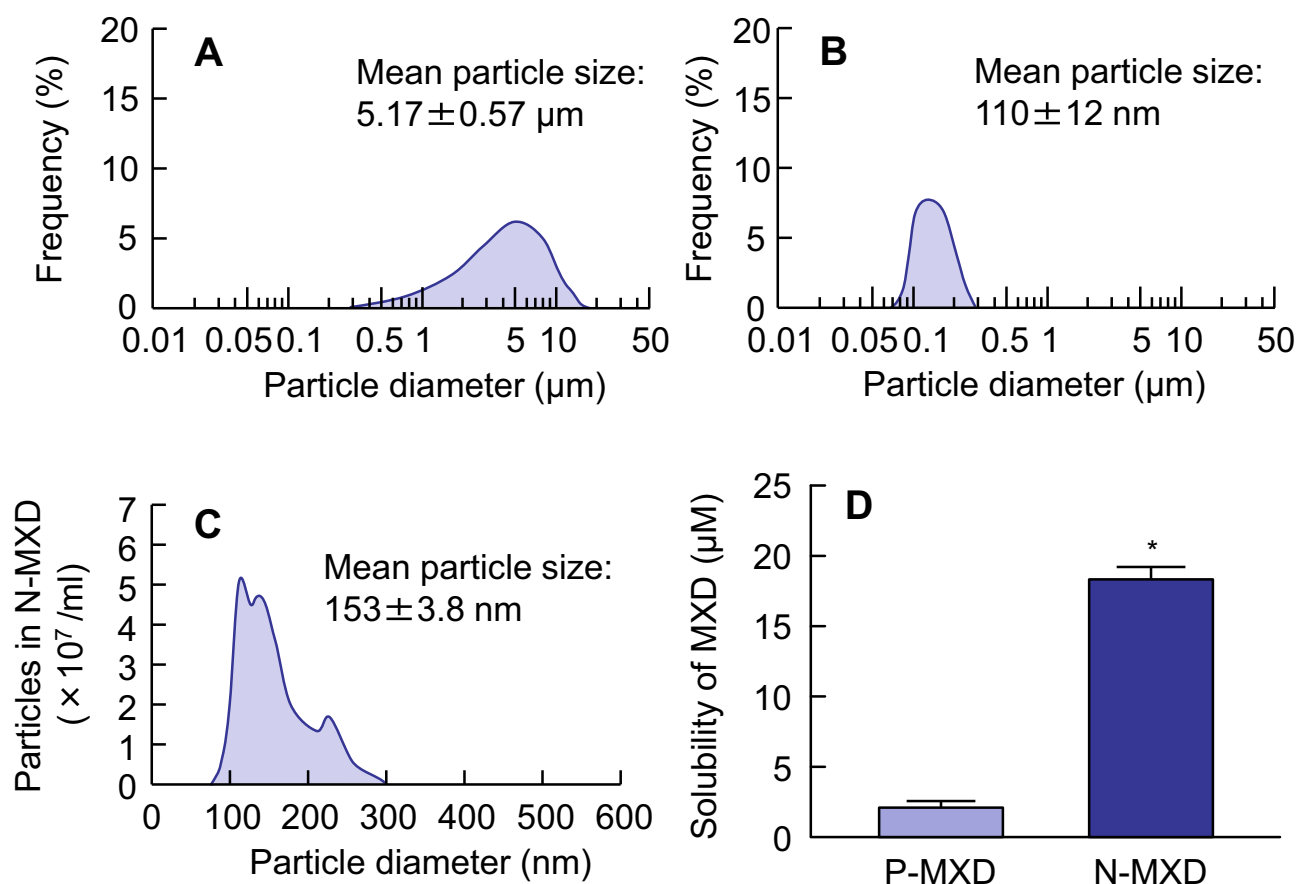


Figure 1 Particle size frequencies and solubility of P-MXD and N-MXD.

Notes: (A) and (B) Particle size frequencies for P-MXD (A) and N-MXD by SALD-71000. (C) Particle size frequencies for N-MXD by NANOSIGHT LM10. (D) Solubility of MXD in P-MXD and N-MXD. $n=6$. * $P<0.05$ vs P-MXD. The particle size of milled MXD was in the nano range (approximately 90 nm–300 nm), and the ratio of solution- and solid-MXD was approximately 2:3 in N-MXD.

Abbreviations: MXD, minoxidil; N-MXD, formulation based on minoxidil nanoparticles; P-MXD, formulation based on minoxidil powder.

Changes In Hair-Growth Factors In C57BL/6 Mice Treated With MXD Formulations

It is known that MXD enhances the expressions of IGF-1 and VEGF, resulting in an increase in hair growth.^{24,25}

In this study, we demonstrated the expression of the mRNA and protein of both IGF-1 and VEGF in the hair bulbs of C57BL/6 mice treated with MXD formulations (Figure 6). The mRNA and protein levels of IGF-1 and VEGF were increased by the MXD formulations and were significantly higher in mice treated with N-MXD rather than CA-MXD. Following the application N-MXD, the IGF-1 and VEGF protein levels in the hair bulbs of C57BL/6 mice were 4.48- and 3.10-fold higher than those of vehicle-applied C57BL/6 mice, and 1.46- and 1.55-fold greater than in CA-MXD-treated C57BL/6 mice.

Discussion

AGA is a common form of hair loss that is observed in both men and women. MXD, used as a first-line therapy for AGA, requires repeated applications for at least 6–8 weeks to recover hair loss. However, the long-term, repeated application of MXD has various adverse effects, such as allergic contact dermatitis, redness, burning, irritation, and scalp dryness. Therefore, new systems to reduce the adverse effects while allowing for effective hair follicle delivery of MXD are crucial for the development for AGA formulas. In this study, we designed N-MXD (a formulation based on MXD NPs) and found that this novel N-MXD shows high hair follicle delivery and provides an effective hair-growth effect in comparison with CA-MXD.

Our group has recently shown that NP dispersions without organic solvents can be prepared by the combination of MC and the mill method,^{16–20} and that drug NP dispersions in purified water containing MC show high dermal permeation

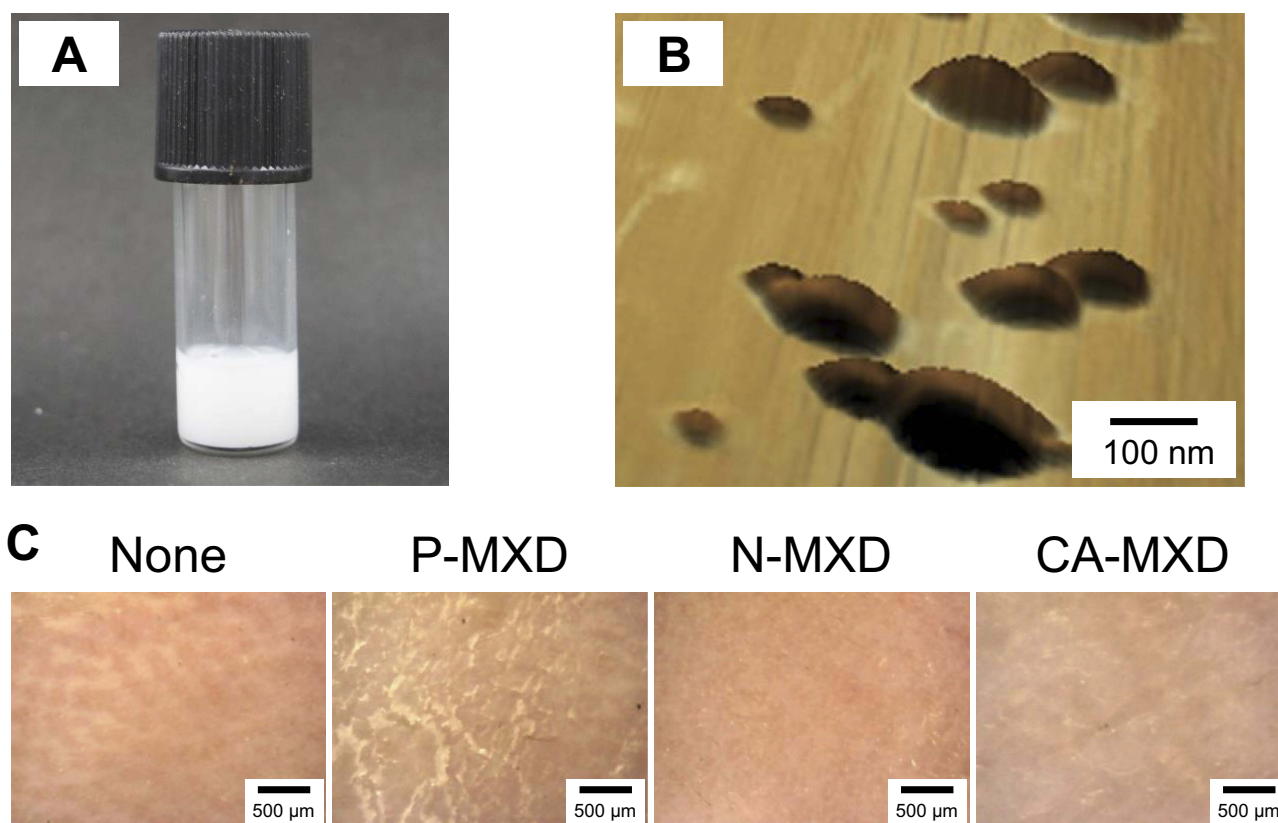


Figure 2 Application of N-MXD to the skin of C57BL/6 mice.

Notes: (A) Digital photo image of N-MXD. (B) AFM images of N-MXD. (C) Microscopic image of the surface of mouse skin 5 mins after application of MXD formulations. Vehicle, mice applied with vehicle for P-MXD and N-MXD. P-MXD, P-MXD-applied mice. N-MXD, N-MXD-applied mice. CA-MXD, CA-MXD-applied mice. MXD NPs are oblong in shape. No redness or MXD powder residue was observed when N-MXD was applied to the skin.

Abbreviations: CA-MXD, commercially available minoxidil formulation; MXD, minoxidil; N-MXD, formulation based on minoxidil nanoparticles; P-MXD, formulation based on minoxidil powder; NPs, nanoparticles.

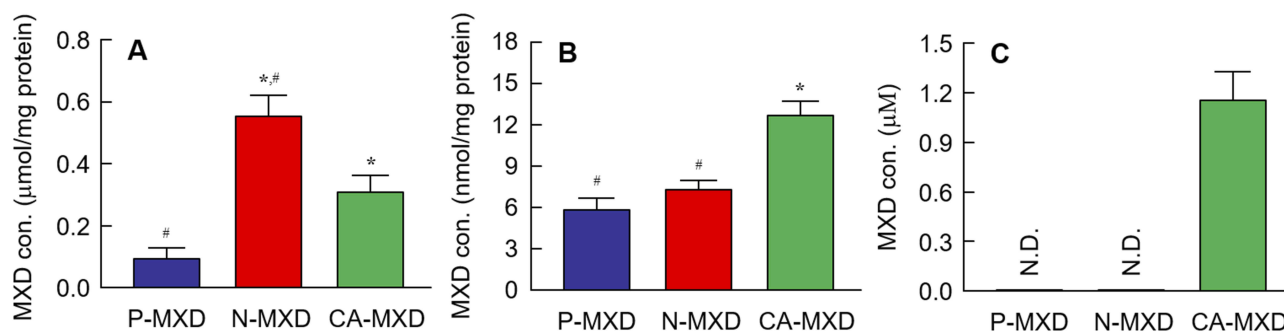


Figure 3 MXD contents in the hair bulb (A), skin tissue (B) and blood (C) of C57BL/6 mice treated with MXD formulations.

Notes: The MXD was applied for 4 h. n=5–7. P-MXD, P-MXD-applied mice. N-MXD, N-MXD-applied mice. CA-MXD, CA-MXD-applied mice. N.D., not detectable. * $P < 0.05$ vs P-MXD for each category. # $P < 0.05$ vs CA-MXD for each category. MXD contents in the skin tissue of N-MXD were lower in CA-MXD. Conversely, the MXD contents in the hair bulbs were higher in N-MXD than in CA-MXD. In the blood, MXD was detected only in CA-MXD.

Abbreviations: CA-MXD, commercially available minoxidil formulation; MXD, minoxidil; N-MXD, formulation based on minoxidil nanoparticles; P-MXD, formulation based on minoxidil powder.

without skin stimulation.^{16–20} In the present work, a novel formulation based on MXD NPs was prepared according to our previous protocol. First, we measured the particle size of MXD after bead mill treatment with MC. The particle size of

the milled-MXD was 90–300 nm (mean particle size 153 ± 3.8 nm, Figure 1C), and the ratio of solid MXD was 61.2% in the N-MXD (Figure 1D). Moreover, the MXD nanoparticles appeared oblong ($2.65 \pm 0.28 \times 10^9$ particles/mL) in the 1%

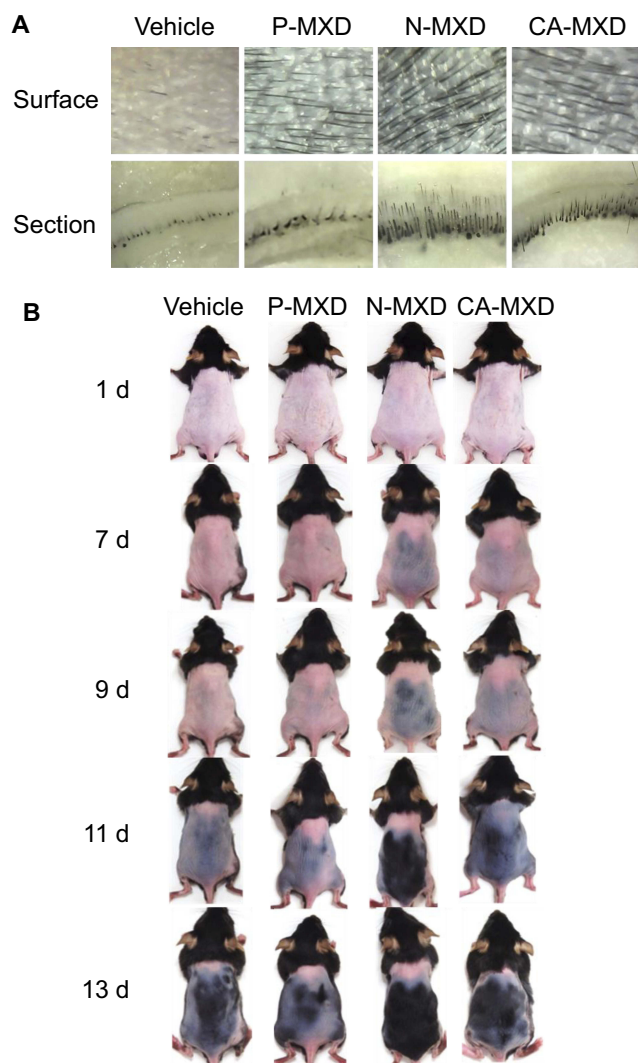


Figure 4 Images showing the hair-growth effects of the repetitive application of MXD formulations in C57BL/6 mice.

Notes: (A) Microscopic image of the skin surface and skin cross-section of C57BL/6 mice skin after 10 d of repetitive application of MXD formulations (once a day). (B) Digital photo image of C57BL/6 mice treated repetitively with MXD formulations for 13 days (once a day). Vehicle, mice applied with the vehicle used to prepare P-MXD and N-MXD. P-MXD, P-MXD-applied mice. N-MXD, N-MXD-applied mice. CA-MXD, CA-MXD-applied mice. Hair growth was promoted by the application of N-MXD and CA-MXD, and the drug efficacy of N-MXD was higher than that of CA-MXD. In addition, no redness or inflammation was observed in skin after the repetitive applications of N-MXD.

Abbreviations: CA-MXD, commercially available minoxidil formulation; MXD, minoxidil; N-MXD, formulation based on minoxidil nanoparticles; P-MXD, formulation based on minoxidil powder.

N-MXD (Figure 2B). We evaluated the condition of the skin to which N-MXD was applied repetitively. No inflammation or MXD powder residue was observed on the treated skin (Figure 2C). These results show that an MXD formulation containing NPs can be prepared by this protocol, and the N-MXD can be used on the skin as a hair formula.

It is important for the effective treatment of AGA that the MXD is delivered into the hair bulbs. Therefore, we

investigated whether the application of N-MXD provides effective delivery of MXD into the hair bulbs through hair follicles. The MXD content in the hair bulbs of mice treated with N-MXD was 6.0- and 1.8-fold higher than in mice treated with P-MXD and CA-MXD, respectively (Figure 3A). We also measured the MXD content in the skin tissue of mice treated with MXD formulations. In contrast to the results for hair bulbs, the MXD content in the skin tissue of mice applied treated with N-MXD was lower in comparison with CA-MXD (Figure 3B). Furthermore, plasma MXD was detected in mice treated with CA-MXD, while in mice treated with N-MXD, no MXD was detectable in the plasma (Figure 3C). CA-MXD contains PG and ethanol as the vehicle (organic solvent), both of which enhance drug skin permeation. In addition, our previous study on the skin permeation of NPs showed that particles over 100 nm in size have difficulty penetrating through the stratum corneum, which acts as a skin barrier, and the permeated NPs dissolve in the skin tissue (only the solution type drug was detected in skin tissue).¹⁸ The drug particle size in the N-MXD used in this study was 90–300 nm. Taken together, the skin permeation from N-MXD is lower than that from CA-MXD (solution type MXD containing organic solvent), and it is possible that the high rate of MXD delivery to the hair bulbs was due to the drug passage through the hair follicle in the case of N-MXD (Figure 7). N-MXD treatment may minimize MXD distribution in normal tissues resulting in high drug efficacy.

Next, we investigated the effect of MXD formulations on hair growth. It is important to choose a relevant model for studies of AGA therapy. The strict coupling of follicular melanogenesis and hair follicle cycling leads to characteristic changes in skin pigmentation during anagen development, and the truncal pigmentation of C57/BL6 mice is entirely dependent on their follicular melanocytes.²⁶ Therefore, C57BL/6 mice have been used to investigate hair-growth effects.²⁶ In this study, we selected C57BL/6 mice as the model of hair follicle regrowth, since their truncal pigmentation is produced only during anagen,²² and the dorsal hair in these mice also has a time-synchronized growth cycle.²¹ Hair growth was promoted by the repetitive application of N-MXD, and the AUC for N-MXD was 1.38- and 1.14-fold higher than those for Vehicle and CA-MXD, respectively (Figures 4 and 5).

We also measured changes in the expression level of proteins involved in hair growth in C57BL/6 mice treated repetitively with MXD formulations using quantitative real-time RT-PCR and ELISA methods. It is known that

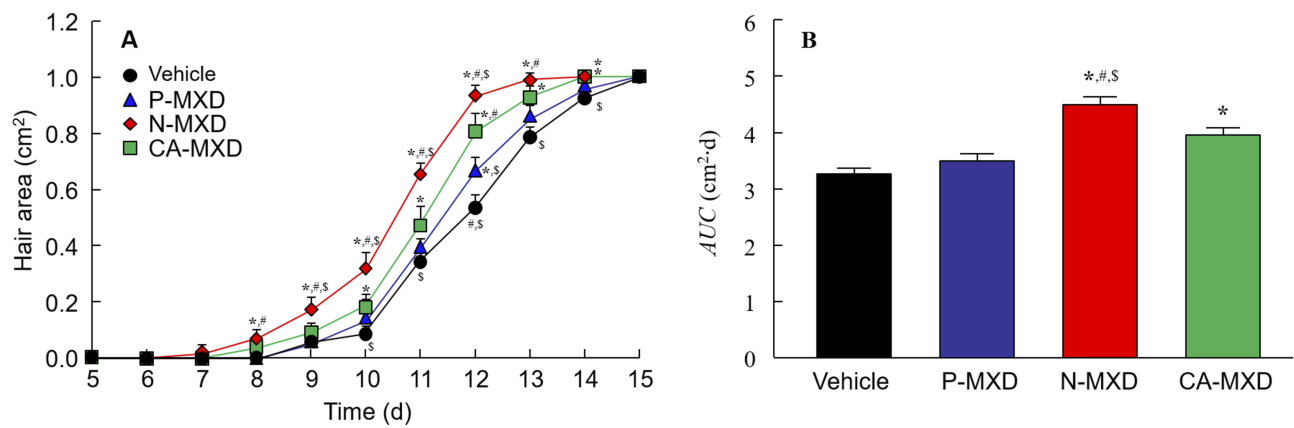


Figure 5 Effect of the repetitive application of MXD on hair growth in C57BL/6 mice.

Notes: (A) and (B) Changes in hair area (A) and AUC (B) in C57BL/6 mice treated with repetitive applications of MXD formulations (once a day). Vehicle, mice treated with the vehicle used to prepare P-MXD and N-MXD. P-MXD, P-MXD-applied mice. N-MXD, N-MXD-applied mice. CA-MXD, CA-MXD-applied mice. n=5–8. * $P < 0.05$ vs Vehicle for each category. # $P < 0.05$ vs P-MXD for each category. § $P < 0.05$ vs CA-MXD for each category. Hair growth was observed from 7 days after the application of N-MXD, and the AUC of N-MXD was significantly higher than those of P-MXD and CA-MXD.

Abbreviations: AUC, area under the hair zone-time curve; CA-MXD, commercially available minoxidil formulation; MXD, minoxidil; N-MXD, formulation based on minoxidil nanoparticles; P-MXD, formulation based on minoxidil powder.

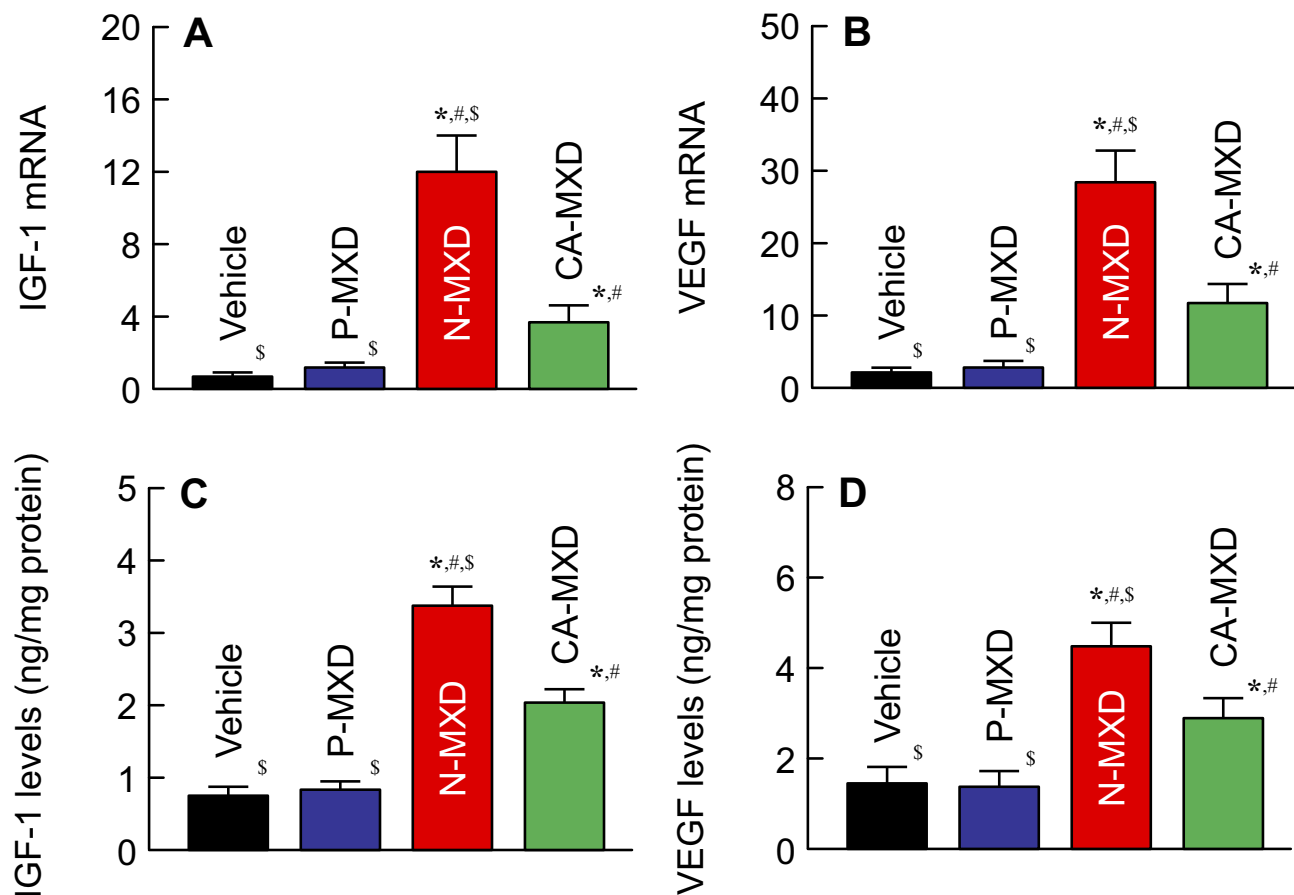


Figure 6 Changes in IGF-1 and VEGF in the hair bulbs of C57BL/6 mice treated with MXD formulations.

Notes: (A) and (B) Expression of IGF-1 (A) and VEGF (B) mRNA in mice after 10 days of repetitive applications of MXD formulations. Vehicle, mice treated with the vehicle used to prepare P-MXD and N-MXD. P-MXD, P-MXD-applied mice. N-MXD, N-MXD-applied mice. CA-MXD, CA-MXD-applied mice. n=5–7. * $P < 0.05$ vs Vehicle for each category. # $P < 0.05$ vs P-MXD for each category. § $P < 0.05$ vs CA-MXD for each category. The mRNA and protein levels of IGF-1 and VEGF were enhanced by the repetitive application of N-MXD and CA-MXD, and the enhanced IGF-1 and VEGF levels were significantly higher in the N-MXD than in CA-MXD.

Abbreviations: CA-MXD, commercially available minoxidil formulation; IGF-1, insulin-like growth factor-1; MXD, minoxidil; N-MXD, formulation based on minoxidil nanoparticles; P-MXD, formulation based on minoxidil powder; VEGF, vascular endothelial growth factor.

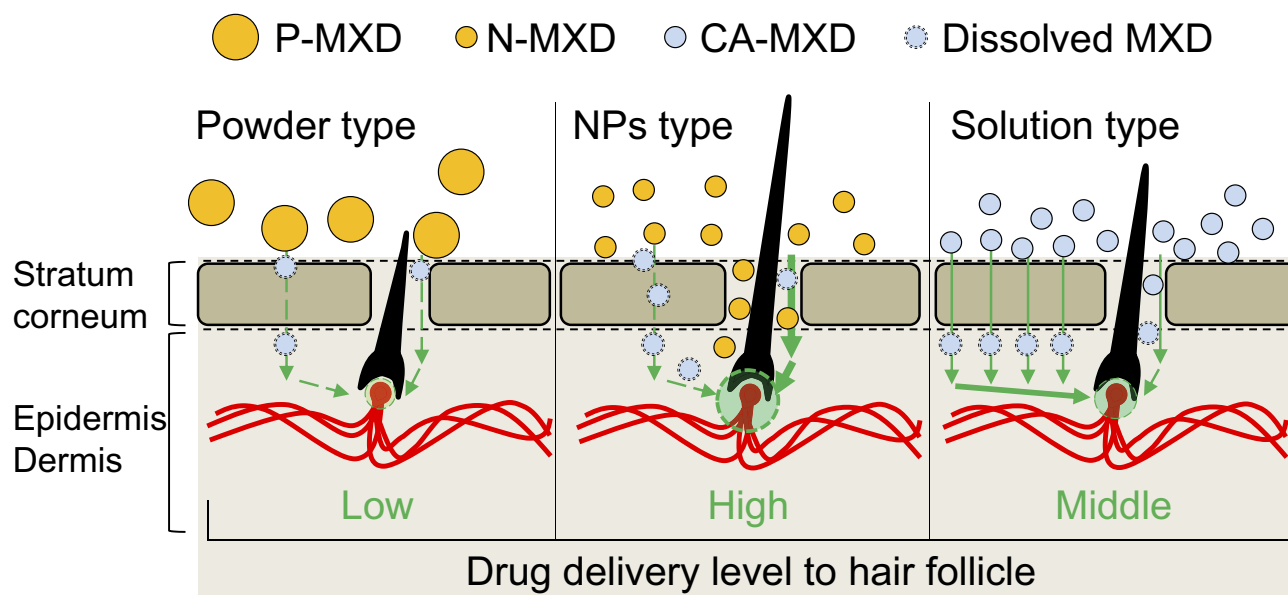


Figure 7 Scheme for drug delivery into the hair bulb for P-MXD (powder type), N-MXD (NPs type), and CA-MXD (solution type).

Abbreviations: CA-MXD, commercially available minoxidil formulation; MXD, minoxidil; N-MXD, formulation based on minoxidil nanoparticles; P-MXD, formulation based on minoxidil powder; NPs, nanoparticles.

IGF-1 activates cells in the hair root and suppresses the catagen and telogen phases of hair growth cycle.²⁷ On the other hand, VEGF, another factor related to hair growth, triggers hair growth, angiogenesis, and vasculogenesis.²⁸ In addition, it has been reported that treatment with MXD enhances these factors in C57BL/6 mice.^{24,25} From these findings, we selected IGF-1 and VEGF as the target proteins used to measure drug efficacy in this study. The mRNA and protein levels of IGF-1 and VEGF increased in response to the application of CA-MXD to 2.71- and 2.01-fold those of vehicle-treated C57BL/6 mice (Figure 6C and 6D). These results support the previous studies showing the enhancement of IGF-1 and VEGF by MXD.^{24,25} In addition, we compared the IGF-1 and VEGF levels between C57BL/6 mice treated repetitively with CA-MXD and N-MXD. The IGF-1 and VEGF protein levels in the hair bulbs of N-MXD-treated C57BL/6 mice were 1.46- and 1.55-fold those of the CA-MXD-treated C57BL/6 mice (Figure 6). Since the MXD contents in the hair bulbs of mice treated with N-MXD were 1.8-fold higher than in mice treated with CA-MXD (Figure 3A), the data suggest that the higher IGF-1 and VEGF levels were caused by the higher MXD content in the hair bulb.

Further studies are needed to clarify the stability and hair follicle delivery of MXD NPs, and clarify any adverse effects or stimulation that may result from long-term use. In addition, it is important to include more controls/comparisons, such as MXD gels, in the

in vivo study. Therefore, we are planning to measure particle frequency and skin inflammation following long-term treatment using transmission electron microscope, dynamic light scattering, and immunohistochemical methods.

Conclusion

We designed a novel nanomedicine based on MXD NPs and showed that N-MXD can deliver MXD into hair bulbs via hair follicles and that the therapeutic efficiency for hair growth is higher than that for CA-MXD. In addition, skin toxicity may be low, since N-MXD is prepared without organic solvents, such as PG and ethyl alcohol. These findings provide significant information to design novel therapeutic drugs for AGA patients.

Disclosure

Dr. Yoshihiro Oaku, Akinari Abe and Tohru Nagahama work for Taisho Pharmaceutical Co., Ltd. The authors report no other conflicts of interest in this work.

References

1. Ellis JA, Sinclair RD. Male pattern baldness: current treatments, future prospects. *Drug Discov Today*. 2008;13:791–797. doi:10.1016/j.drudis.2008.05.010
2. Khan MZU, Khan SA, Ubaid M, Shah A, Kousar R, Murtaza G. Finasteride topical delivery systems for androgenetic alopecia. *Curr Drug Deliv*. 2018;15:1100–1111. doi:10.2174/1567201815666180124112905

3. Mura S, Manconi M, Sinico C, Valenti D, Fadda AM. Penetration enhancer-containing vesicles (PEVs) as carriers for cutaneous delivery of minoxidil. *Int J Pharm.* 2009;380:72–79. doi:10.1016/j.ijpharm.2009.06.040
4. Aronson JK. Minoxidil. In: Aronson JK, editor. *Meyley's Side Effects of Drugs: The International Encyclopedia of Adverse Drug Reactions and Interactions*. Amsterdam: Elsevier; 2006:2354–2356.
5. Pavithran K. Erythema multiforme following topical minoxidil. *Indian J Dermatol Venerol Leprol.* 1993;59:313–314.
6. Wagner L, Kenreigh C. Minoxidil. In: Enna SJ, David BB, editors. *xPharm: The Comprehensive Pharmacology Reference*. Amsterdam: Elsevier; 2007:1–5.
7. Padois K, Cantieni C, Bertholle V, Bardel C, Pirot F, Falson F. Solid lipid nanoparticles suspension versus commercial solutions for dermal delivery of minoxidil. *Int J Pharm.* 2011;416:300–304. doi:10.1016/j.ijpharm.2011.06.014
8. Knorr F, Lademann J, Patzelt A, Sterry W, Blume-Peytavi U, Vogt A. Follicular transport route—research progress and future perspectives. *Eur J Pharm Biopharm.* 2009;71:173–180. doi:10.1016/j.ejpb.2008.11.001
9. Lademann J, Richter H, Teichmann A, et al. Nanoparticles – an efficient carrier for drug delivery into the hair follicles. *Eur J Pharm Biopharm.* 2007;66:159–164. doi:10.1016/j.ejpb.2006.10.019
10. Prow TW, Grice JE, Lin LL, et al. Nanoparticles and microparticles for skin drug delivery. *Adv Drug Deliv Rev.* 2011;63:470–491. doi:10.1016/j.addr.2011.01.012
11. Yoon G, Park JW, Yoon I-S. Solid lipid nanoparticles (SLNs) and nanostructured lipid carriers (NLCs): recent advances in drug delivery. *J Pharm Investig.* 2013;43:353–362. doi:10.1007/s40005-013-0087-y
12. Aljuffali IA, Pan TL, Sung CT, Chang SH, Fang JY. Anti-PDGF receptor β antibody-conjugated squarticles loaded with minoxidil for alopecia treatment by targeting hair follicles and dermal papilla cells. *Nanomedicine.* 2015;11:1321–1330. doi:10.1016/j.nano.2015.04.009
13. Gelfuso GM, Barros MA, Delgado-Charro MB, Guy RH, Lopez RF. Iontophoresis of minoxidil sulphate loaded microparticles, a strategy for follicular drug targeting? *Colloids Surf B Biointerfaces.* 2015;134:408–412. doi:10.1016/j.colsurfb.2015.07.031
14. Gelfuso GM, Gratieri T, Simão PS, de Freitas LA, Lopez RF. Chitosan microparticles for sustaining the topical delivery of minoxidil sulphate. *J Microencapsul.* 2011;28:650–658. doi:10.3109/02652048.2011.604435
15. Matos BN, Reis TA, Gratieri T, Gelfuso GM. Chitosan nanoparticles for targeting and sustaining minoxidil sulphate delivery to hair follicles. *Int J Biol Macromol.* 2015;75:225–229. doi:10.1016/j.ijbiomac.2015.01.036
16. Nagai N, Ito Y, Okamoto N, Shimomura Y. A nanoparticle formulation reduces the corneal toxicity of indomethacin eye drops and enhances its corneal permeability. *Toxicology.* 2014;319:53–62. doi:10.1016/j.tox.2014.02.012
17. Nagai N, Yoshioka C, Ito Y, Funakami Y, Nishikawa H, Kawabata A. Intravenous administration of cilostazol nanoparticles ameliorates acute ischemic stroke in a cerebral ischemia/reperfusion-induced injury model. *Int J Mol Sci.* 2015;16:29329–29344. doi:10.3390/ijms161226166
18. Nagai N, Ogata F, Otake H, Nakazawa Y, Kawasaki N. Design of a transdermal formulation containing raloxifene nanoparticles for osteoporosis treatment. *Int J Nanomedicine.* 2018;13:5215–5229. doi:10.2147/IJN.S173216
19. Nagai N, Ogata F, Ishii M, et al. Involvement of endocytosis in the transdermal penetration mechanism of ketoprofen nanoparticles. *Int J Mol Sci.* 2018;19:pii:E2138. doi:10.3390/ijms19072138
20. Nagai N, Iwamae A, Tanimoto S, Yoshioka C, Ito Y. Pharmacokinetics and anti-inflammatory effect of a novel gel system containing ketoprofen solid nanoparticles. *Biol Pharm Bull.* 2015;38:1918–1924. doi:10.1248/bpb.b15-00567
21. Müller-Röver S, Handjiski B, van der Veen C, et al. A comprehensive guide for the accurate classification of murine hair follicles in distinct hair cycle stages. *J Invest Dermatol.* 2001;117:3–15. doi:10.1046/j.0022-202x.2001.01377.x
22. Slominski A, Paus R, Plonka P, et al. Melanogenesis during the anagen-catagen-telogen transformation of the murine hair cycle. *J Invest Dermatol.* 1994;102:862–869. doi:10.1111/1523-1747.ep12382606
23. Nagai N, Ogata F, Otake H, Nakazawa Y, Kawasaki N. Energy-dependent endocytosis is responsible for drug transcorneal penetration following the instillation of ophthalmic formulations containing indomethacin nanoparticles. *Int J Nanomedicine.* 2019;14:1213–1227. doi:10.2147/IJN.S196681
24. Kim MJ, Lim C, Lee JY, Im KR, Yoon KS, Song JM. Visible-to-near IR quantum dot-based hypermulticolor high-content screening of herbal medicines for the efficacy monitoring of hair growth promotion and hair loss inhibition. *J Biomol Screen.* 2013;18:462–473. doi:10.1177/1087057112464574
25. Park KS, Park DH. Comparison of Saccharina japonica-Undaria pinnatifida mixture and minoxidil on hair growth promoting effect in mice. *Arch Plast Surg.* 2016;43:498–505. doi:10.5999/aps.2016.43.6.498
26. Zhang Y, Chen S, Qu F, Su G, Zhao Y. In vivo and in vitro evaluation of hair growth potential of Cacumen Platycladi, and GC-MS analysis of the active constituents of volatile oil. *J Ethnopharmacol.* 2019;238:111835. doi:10.1016/j.jep.2019.111835
27. Angunsri N, Taura A, Nakagawa T, et al. Insulin-like growth factor 1 protects vestibular hair cells from aminoglycosides. *Neuroreport.* 2011;22:38–43. doi:10.1097/WNR.0b013e32834273e9
28. Yano K, Brown LF, Detmar M. Control of hair growth and follicle size by VEGF-mediated angiogenesis. *J Clin Invest.* 2001;107:409–417. doi:10.1172/JCI11317

International Journal of Nanomedicine

Publish your work in this journal

The International Journal of Nanomedicine is an international, peer-reviewed journal focusing on the application of nanotechnology in diagnostics, therapeutics, and drug delivery systems throughout the biomedical field. This journal is indexed on PubMed Central, MedLine, CAS, SciSearch®, Current Contents®/Clinical Medicine,

Submit your manuscript here: <https://www.dovepress.com/international-journal-of-nanomedicine-journal>

Dovepress

Journal Citation Reports/Science Edition, EMBASE, Scopus and the Elsevier Bibliographic databases. The manuscript management system is completely online and includes a very quick and fair peer-review system, which is all easy to use. Visit <http://www.dovepress.com/testimonials.php> to read real quotes from published authors.